Radiotherapy and Oncology 137 (2019) 45–54

Contents lists available at ScienceDirect

Radiotherapy and Oncology

journal homepage: www.thegreenjournal.com

Original Article

DNA damage accumulation during fractionated low-dose radiation compromises hippocampal neurogenesis

Zoé Schmal [a], Anna Isermann [a], Daniela Hladik [b], Christine von Toerne [c], Soile Tapio [b], Claudia E. Rübe [a,*]

[a] Department of Radiation Oncology, Saarland University, Homburg/Saar; [b] Institute of Radiation Biology, Helmholtz Zentrum München, German Research Center for Environmental Health GmbH; and [c] Research Unit Protein Science, Helmholtz Zentrum München, German Research Center for Environmental Health GmbH, Neuherberg, Germany

ARTICLE INFO

Article history:
Received 10 January 2019
Received in revised form 22 March 2019
Accepted 18 April 2019
Available online 4 May 2019

Keywords:
Neurogenesis
Hippocampus
Low-dose radiation
Normal tissue toxicity
DNA double-strand breaks
DNA damage foci

ABSTRACT

Background and purpose: High-precision radiotherapy is an effective treatment modality for tumors. Intensity-modulated radiotherapy techniques permit close shaping of high doses to tumors, however healthy organs outside the target volume are repeatedly exposed to low-dose radiation (LDR). The inherent vulnerability of hippocampal neurogenesis is likely the determining factor in radiation-induced neurocognitive dysfunctions. Using preclinical *in-vivo* models with daily LDR we attempted to precisely define the pathophysiology of radiation-induced neurotoxicity.

Material and methods: Genetically defined mouse strains with varying DNA repair capacities were exposed to fractionated LDR (5×/10×/15×/20×0.1 Gy) and dentate gyri from juvenile and adult mice were analyzed 72 h after last exposure and 1, 3, 6 months after 20 × 0.1 Gy. To examine the impact of LDR on neurogenesis, persistent DNA damage was assessed by quantifying 53BP1-foci within hippocampal neurons. Moreover, subpopulations of neuronal stem/progenitor cells were quantified and dendritic arborization of developing neurons were assessed. To unravel molecular mechanisms involved in radiation-induced neurotoxicity, hippocampi were analyzed using mass spectrometry-based proteomics and affected signaling networks were validated by immunoblotting.

Results: Radiation-induced DNA damage accumulation leads to progressive decline of hippocampal neurogenesis with decreased numbers of stem/progenitor cells and reduced complexities of dendritic architectures, clearly more pronounced in repair-deficient mice. Proteome analysis revealed substantial changes in neurotrophic signaling, with strong suppression directly after LDR and compensatory upregulation later on to promote functional recovery.

Conclusion: Hippocampal neurogenesis is highly sensitive to repetitive LDR. Even low doses affect signaling networks within the neurogenic niche and interrupt the dynamic process of generation and maturation of neuronal stem/progenitor cells.

Radiotherapy is an effective treatment modality for patients of all ages with malignant and benign tumors. With intensity-modulated radiotherapy (IMRT) multiple photon-beams from different directions and with adjusted intensities permit close shaping of radiation dose to target volumes, thereby delivering high doses to tumors while sparing specific risk regions. However, with IMRT large volumes of non-targeted brain regions are exposed to daily low-dose radiation (LDR), which may adversely affect neurocognitive functions. Due to improved treatment techniques, young cancer patients survive longer, and can therefore experience the debilitating late-effects of radiotherapy, including attention deficits and learning difficulties later in life [1].

Accumulating data indicate that ionizing radiation (IR) not only affects mature neuronal networks, but particularly proliferation and differentiation of neuronal stem/progenitor cells [2–7]. The generation of new neurons from largely quiescent neural stem cells occurs throughout life in the subgranular zone (SGZ) of hippocampal dentate gyrus. Neural stem cells give rise to transiently dividing precursor cells, that migrate into the granule cell layer, and differentiate into mature neurons which become functionally integrated into hippocampal circuitry [8]. Specific markers expressed in distinct cell types during different stages of neurogenesis permit to identify subpopulations within the complex hippocampal architecture. Transcription-factor SOX2 (SRY[sex-determining-region-Y]box2) plays important roles in maintaining neural stem/progenitor cell properties [9]. DCX (doublecortin) is expressed in migrating neuroblasts and immature neurons [10]. NeuN is used as specific marker for mature post-mitotic neurons [11]. Aging of the brain

* Corresponding author at: Department of Radiation Oncology, Saarland University, Kirrbergerstrasse Building 6.5, 66421 Homburg/Saar, Germany.
E-mail address: claudia.ruebe@uks.eu (C.E. Rübe).

https://doi.org/10.1016/j.radonc.2019.04.021
0167-8140/

is marked by major decrease in the number of new neurons generated in hippocampal dentate gyrus [12]. This age-dependent decline of neurogenesis leads to reduced regeneration capacity and is caused by cell-intrinsic and cell-extrinsic signals within the neurogenic niche [13]. In hippocampal microenvironment, *cAMP response element-binding* (CREB) protein plays critical roles in proliferation, survival and differentiation of neuronal stem/progenitor cells [14]. In response to genotoxic insults, CREB-activation leads to expression of neuroprotective factors, such as *brain-derived neurotrophic factor* (BNDF) [15] and *activity-regulated cytoskeleton-associated protein* (ARC) [16], and contributes to protection and survival of newborn neurons.

Following exposure to ionizing radiation, cells incur DNA lesions that jeopardize genomic integrity, with double-strand breaks (DSBs) being the most critical DNA lesions. During DNA damage response (DDR) the formation of large aggregates of sensor/mediator proteins at DSB sites can be visualized as nuclear foci by immunofluorescence microscopy (IFM) [17]. Within these foci, activation of mediator proteins, most notably DNA-PK and Ataxia- Telangiectasia-Mutated (ATM), transduce DSB signals to numerous downstream effectors, setting the scene for DSB repair [18]. Mutations in these sensor/mediator proteins have been shown to contribute to pronounced radiosensitivity. Severe-combined-immunodeficiency (*SCID*) is caused by gene mutations encoding DNA-PKcs, resulting in defective V(D)J-recombination and extreme radiosensitivity [19]. ATM is mutated in the Ataxia-Telangiectasia (AT) syndrome, which is characterized by progressive neurodegeneration, telangiectasia, immunodeficiency, and marked radiosensitivity [18].

Radiation-induced accumulation of DNA damage in neuronal stem/progenitor cells may have profound impact on genomic integrity and may contribute to impairment of stem cell functions, with loss of self-renewal and differentiation capacities [20,21]. In the current experimental study, acute and long-term effects of fractionated LDR on the complex process of adult neurogenesis were characterized to evaluate the impact of genomic damage on neuronal stem cell behaviour.

Materials and methods

Mouse strains

C57BL/6 mice (Charles River Laboratories, Sulzfeld, Germany) were used as DNA repair-proficient wild-type (WT) mice; homogenous *ATM*$^{-/-}$ (129S6/SvEvTac-*Atm*^{tm1Awb}/J; Jackson Laboratory) and *DNA-PKcs*$^{-/-}$ mice (CB17/Icr-Prkdc^{scid}/Rj; Janvier, St. Berthevin Cedex, France.) served as DNA repair-deficient AT and SCID mice. Only male mice were used for these studies and housed in groups in IVC cages under standard laboratory conditions.

Animal irradiation

Whole-body radiation (0.1 Gy) was performed at linear accelerators (Artiste™, Siemens) as described previously [22]. Juvenile and young adult C57BL/6 mice (age P11 or P56 at start of LDR experiments) were daily irradiated from Monday to Friday for 1, 2, 3 or 4 weeks. 72 h after 5×, 10×, 15×, 20× fractions, and 1, 3, 6 months after 20× fractions animals were anesthetized prior to tissue collection. Adult AT and SCID mice received 1×, 10×, or 20× fractions and brain tissue was analyzed 72 h after the last exposure. Brain tissues of ≥3 mice per age, per strain and per time-point were analyzed compared to age-matched, non-irradiated controls. Studies were approved by Medical Sciences Animal Care and Use Committee of Saarland University.

Immunofluorescence microscopy

Formalin-fixed brain tissues were embedded in paraffin and cut into 4-μm coronal sections from Bregma −1.9 mm onwards. Paraffin was removed in xylene and sections were rehydrated in decreasing alcohol concentrations. Tissues were boiled in citrate buffer and pre-incubated with Roti™-Immunoblock (Carl Roth, Karlsruhe, Germany), incubated with primary antibodies (53BP1, Bethyl Laboratories, Montgomery, TX, USA; NeuN, Merck Millipore, Darmstadt, Germany; DCX, SantaCruz, Dallas, TX, USA; SOX2, Abcam, Cambridge, UK) followed by incubation with Alexa-Fluor-488 or Alexa-Fluor-568 secondary antibodies (Invitrogen, Karlsruhe, Germany). Finally, sections were mounted in VECTAshield™ with 4′,6-diamidino-2-phenylindole (DAPI; Vector Laboratories, Burlingame, CA, USA). Nikon Eclipse Ni-E epifluorescence microscope equipped with charge-coupled-device camera and acquisition software (NIS-Elements, Nikon, Düsseldorf, Germany) was used to capture fluorescence images. 53BP1-foci were quantified in NeuN-positive neurons until at least 40 cells and 40 foci were registered per tissue sample. In DCX-stained sections overview tiles were acquired with ZEISS AxioScan, whereupon detailed 3D-image z-stacks were acquired with higher magnification (60×) using LSM-800-AiryScan. DCX^{+} cells were quantified in entire granule cell layers (GCL), SOX2^{+} cells were captured exclusively in subgranular zones (SGZ). Cell numbers and dentritic arborization (evaluated by measuring DCX^{+} areas) were reported in relation to GCL size, evaluated by NIS-elements software.

Protein isolation

Snap-frozen hippocampi were pulverized and resuspended in RIPA enriched with phosphatase/protease inhibitors. After sonification, suspensions were incubated and centrifugated and protein concentrations were determined using BCA method according to manufacturer's instructions [23].

Mass spectrometry-based proteome analysis:

Measurements were performed on QExactive mass-spectrometer (Thermo Fisher Scientific Inc.) coupled to UltiMate™3000 nano-RSLC (Thermo Fisher Scientific Inc.) as described previously [24].

Label-free proteomic analysis with progenesis QI

MS-spectra were further analyzed with Progenesis QI software (Nonlinear Dynamics, Water, Newcastle upon Tyne, UK) for label-free quantification as described before [24].

Bioinformatics

To identify radiation-affected signaling pathways, differentially regulated proteins were imported into Ingenuity Pathway Analysis (IPA, QIAGEN Redwood City, www.qiagen.com/ingenuity).

Western Blot

Samples were denatured with Lämmli-buffer and proteins were separated using 4–12% gradient gels and blotted onto nitrocellulose membranes. Membranes were blocked and incubated with first antibodies. After washing membranes were incubated with HPR-secondary antibodies and visualized with chemiluminescence detection. Protein bands were quantified with Image-J software. Ponceau staining served as internal loading control.

Statistical analysis

Differences in 53BP1-foci, DCX^+ and $SOX2^+$ cells between irradiated versus non-irradiated hippocampi were assessed using unpaired Student's *t*-test (GraphPad Software, La Jolla, CA, USA). Differences were considered statistically significant at *p*-values ≤ 0.05. Filtering criteria for proteomics analyses: (i) significance for fold-change (ratio irradiated to non-irradiated) ≥ 1.30 or ≤ 0.770; (ii) $p \leq 0.05$; (iii) identification by ≥ 2UP. For immunoblotting, differences in protein expression were considered to be significant if $p \leq 0.05$ (unpaired Student's t-test). Error bars were calculated as standard error of the mean (SEM).

Data availability

Raw MS-data are available in https://www.storedb.org/store_v3/study.jsp?studyId=1107

Results

53BP1-foci accumulation in hippocampal neurons during and after LDR

Double-staining for NeuN and 53BP1 was used to quantify DNA damage foci in mature, post-mitotic neurons located in hippocampal dentate gyrus of WT mice (Fig. 1). Only low 53BP1-foci levels (~0.03 foci/cell) were observed in non-irradiated controls (Fig. 1A, left panel). Directly after single-dose exposure to 0.1 Gy, approximately 1 focus/cell was induced at 0.1 h post-IR (Fig. 1A, middle panel). Following fractionated LDR (20×0.1 Gy, 72 h post-IR) the number of persisting foci was higher in hippocampal neurons compared to non-irradiated WT mice (Fig. 1A, right panel). To assess possible accumulation of persisting 53BP1-foci during fractionated LDR, juvenile and adult WT mice were examined 72 h after exposure to 5×, 10×, 15×, or 20× fractions of 0.1 Gy, compared to non-irradiated, age-matched controls (Fig. 1B). The number of persisting 53BP1-foci increased significantly in juvenile and adult WT mice during fractionated LDR, with the maximum at 1 m post-IR (juvenile: 0.092 ± 0.0046 foci/cell; adult: 0.075 ± 0.004 foci/cell; Fig. 1B). Subsequently, numbers of radiation-induced foci decreased gradually, but failed to return to baseline levels observed in non-irradiated controls, even six months after the last exposure (Fig. 1B). Due to the limited numbers of DCX^+ neuroprogenitors, it was not feasible to perform the quantitative analysis of 53BP1-foci in older mice. However, in the juvenile dentate gyrus we found similar kinetics of 53BP1-foci formation and disappearance in DCX^+ neuroprogenitors.

Radiation-induced DNA damage usually induces cell-cycle arrest and apoptosis. Ki-67 immunostaining was performed to analyze the proliferative potential of neuronal precursors in the hippocampus (Suppl.1A). In juvenile WT mice the proportion of $Ki67^+$ cells in the SGZ of dentate gyrus was significantly decreased 72 h after 20×0.1 Gy and, notably, at all later time-points (Suppl.1A, inset), indicating that proliferation of neurogenic precursors was compromised by repetitive LDR in the long term. In contrast, numbers of $Ki67^+$ cells in adult WT mice were not significantly affected by LDR (Fig. 1A). To test whether this moderate DNA damage caused apoptosis in immature DCX^+ neurons, Caspase-3 expression was analyzed (Suppl.1B). Quantification of Caspase-3 immunostaining showed no significant increase in apoptotic cells in juvenile or adult hippocampi 72 h after 20×0.1 Gy (Suppl.1B). In summary, these results indicate that even low doses of ionizing radiation may negatively influence neuronal proliferation in immature brain.

Cellular response of DCX^+ neuroprogenitors to fractionated LDR

Using high-resolution imaging we analyzed the morphology of DCX^+ neuroprogenitors to examine the effects of LDR on the development and maturation of their dendritic tree (Fig. 2A). In hippocampal dentate gyrus of non-irradiated brain, DCX^+ cell bodies were primarily located in SGZ, while their dendrites extended radially into the molecular layer (Fig. 2A, left panel). Fractionated LDR resulted in distinct reduction in dendritic arborization with diminished branching, total length and dendritic complexity (Fig. 2B, right panel).

Next, the number of DCX^+ cells was quantified in the SGZ of hippocampal dentate gyrus. In non-irradiated WT mice the physiological age-related decline of hippocampal neurogenesis correlated with decreased levels of DCX^+ neuroprogenitors (Fig. 2B, upper panels). During and after fractionated LDR, the number of DCX^+ neuroprogenitors was significantly lower across all time-points compared to non-irradiated, age-matched controls (Fig. 2B, upper panels). In juvenile WT mice, DCX^+ neuroprogenitors decreased to ~70% during and immediately after fractionated LDR (20×0.1 Gy, 72 h post-IR: 702 ± 26 DCX^+ cells/mm^2; non-IR: 1007 ± 29 DCX^+ cells/mm^2), and stayed at low levels showing ~50% decrease in the long term, compared to non-irradiated aged-matched controls (20×0.1 Gy, 6 m post-IR: 85 ± 4 DCX^+ cells/mm^2; non-IR: 172 ± 11 DCX^+ cells/mm^2). In adult WT mice, radiation-induced decrease in DCX^+ neuroprogenitors was less prominent, showing ≤25% cell loss at early (20×0.1 Gy, 72 h post-IR: 298 ± 11 DCX^+ cells/mm^2; non-IR: 389 ± 8 DCX^+ cells/mm^2) and later time-points (20×0.1 Gy, 3 m post-IR: 147 ± 5 DCX^+ cells/mm^2; non-IR: 189 ± 14 DCX^+ cells/mm^2). Our findings suggest that the high neurogenic potential of developing brain is associated with marked susceptibility to genotoxic stress and may explain age-dependent vulnerability of hippocampal neurogenesis to radiation injury.

Subsequently, DCX^+ areas were measured in hippocampal regions by 2D-image analysis to quantify radiation effects on arborization densities (Fig. 2B, lower panels). During fractionated LDR the percentage of DCX^+ area in juvenile hippocampus declined from ~12% (5×0.1 Gy, 72 h post-IR) to ~6% (20×0.1 Gy, 72 h post-IR), and in adult hippocampus from ~5% (5×0.1 Gy, 72 h post-IR) to ~3% (20×0.1 Gy, 72 h post-IR), correlating with radiation-induced decrease of ≤50% in juvenile and ≤25% in adult hippocampus (Fig. 2B). Following fractionated LDR we observed constant reductions in dendritic arborization with clear decreases of ≤50% in juvenile and ≤25% in adult hippocampus, compared to non-irradiated controls. In summary, these results indicate significant long-lasting effects of repetitive LDR on the number of differentiating DCX^+ neurons and the outgrowth and branching of their dendritic arbors. These radiation effects were even more pronounced in maturing brain of juvenile mice, likely reflecting the higher neurogenic potential leading to increased vulnerability to genotoxic stress.

Cellular response of $SOX2^+$ stem/progenitor cells to fractionated LDR

Transcription-factor SOX2, expressed by slowly proliferating neuroprogenitors, is important in controlling self-renewal and multipotency. In the hippocampus of juvenile and adult WT mice, $SOX2^+$ cells were quantified in the SGZ along the hilus of dentate gyrus (Fig. 3). In juvenile WT mice, numbers of $SOX2^+$ precursors remained stable during LDR, but were significantly reduced at all time-points after LDR with 30–40% decreases compared to non-irradiated, age-matched controls (Fig. 3B, left panel). These temporal dynamics of $SOX2^+$ cells may reflect that genotoxic insults caused by repetitive LDR result in their premature differentiation to replace damaged cells after radiation injury. In adult WT mice,

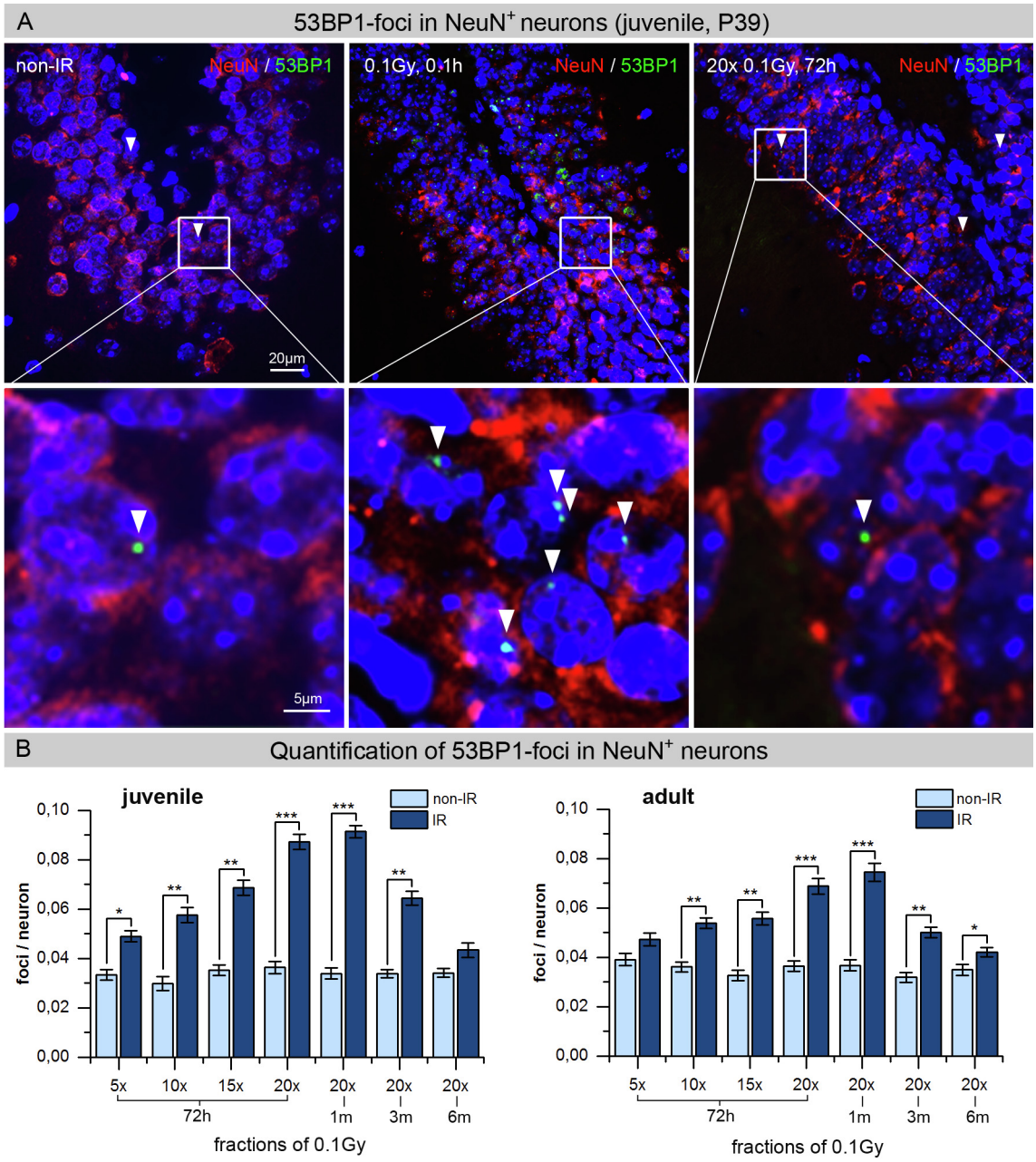

Fig. 1. 53BP1-foci accumulation in neurons during and after fractionated LDR. A: Immunofluorescence imaging of 53BP1-foci (green) in NeuN-positive nuclei (red) of non-irradiated and irradiated hippocampus from repair-proficient juvenile WT mice. Hippocampal neurons of control hippocampus show low 53BP1-foci levels (left panel). At 0.1 h after single-dose exposure to 0.1 Gy the number of foci was clearly increased (~1 focus/cell; middle panel). At 72 h after 20 × 0.1 Gy only few neurons showed persistent 53BP1-foci. Framed regions are shown at higher magnification (600×). Arrow heads mark 53BP1-foci. B: Quantification of radiation-induced 53BP1-foci in NeuN-positive hippocampal neurons. To analyze persistent DNA damage during and after fractionated LDR, numbers of 53BP1-foci per cell were quantified 72 h after 5×, 10×, 15× or 20× fractions of 0.1 Gy and 1, 3, and 6 months after 20 × 0.1 Gy. 53BP1-foci were quantified in hippocampal neurons of juvenile and young adult WT mice and compared to age-matched, non-irradiated controls. Error bars represent SEM, $n \geq 3$; *denotes statistically significant difference compared to non-irradiated control: $^{*}p < 0.05$; $^{**}p < 0.01$; $^{***}p < 0.001$.

the number of SOX2$^+$ stem/progenitor cells *per se* was clearly lower compared to maturing brain, but was not significantly affected by LDR (Fig. 3B, right panel).

Defective DNA damage signaling determines stem cell functionality

ATM and DNA-PKcs are central DDR regulators, but understanding of their downstream signals determining stem cell functionality remains incomplete. Repair-deficient AT and SCID mice showed significantly increased basal levels of 53BP1-foci in neurons of non-irradiated hippocampi compared to WT mice (AT: 0.13 ± 0.02 foci/-cell; SCID: 0.35 ± 0.04 foci/cell) (Fig. 4A). Following fractionated LDR, repair-deficient AT mice showed significantly increased levels of remaining foci after 10 or 20 fractions, with the maximum of 0.66 ± 0.07 foci/cell (20 × 0.1 Gy). Repair-deficient SCID mice showed most pronounced accumulation of unrepaired DNA damage, with 1.70 ± 0.09 foci/cell after 20 × 0.1 Gy (Fig. 4A). Taken together, these elevated foci numbers after LDR reflect prominent DSB repair deficiency of AT and SCID mice.

As neurogenesis is particularly susceptible to genotoxic stress, neuronal stem/progenitor cells were quantified in SGZ of hippocampal dentate gyrus (Fig. 4B). In AT mice numbers of DCX$^+$

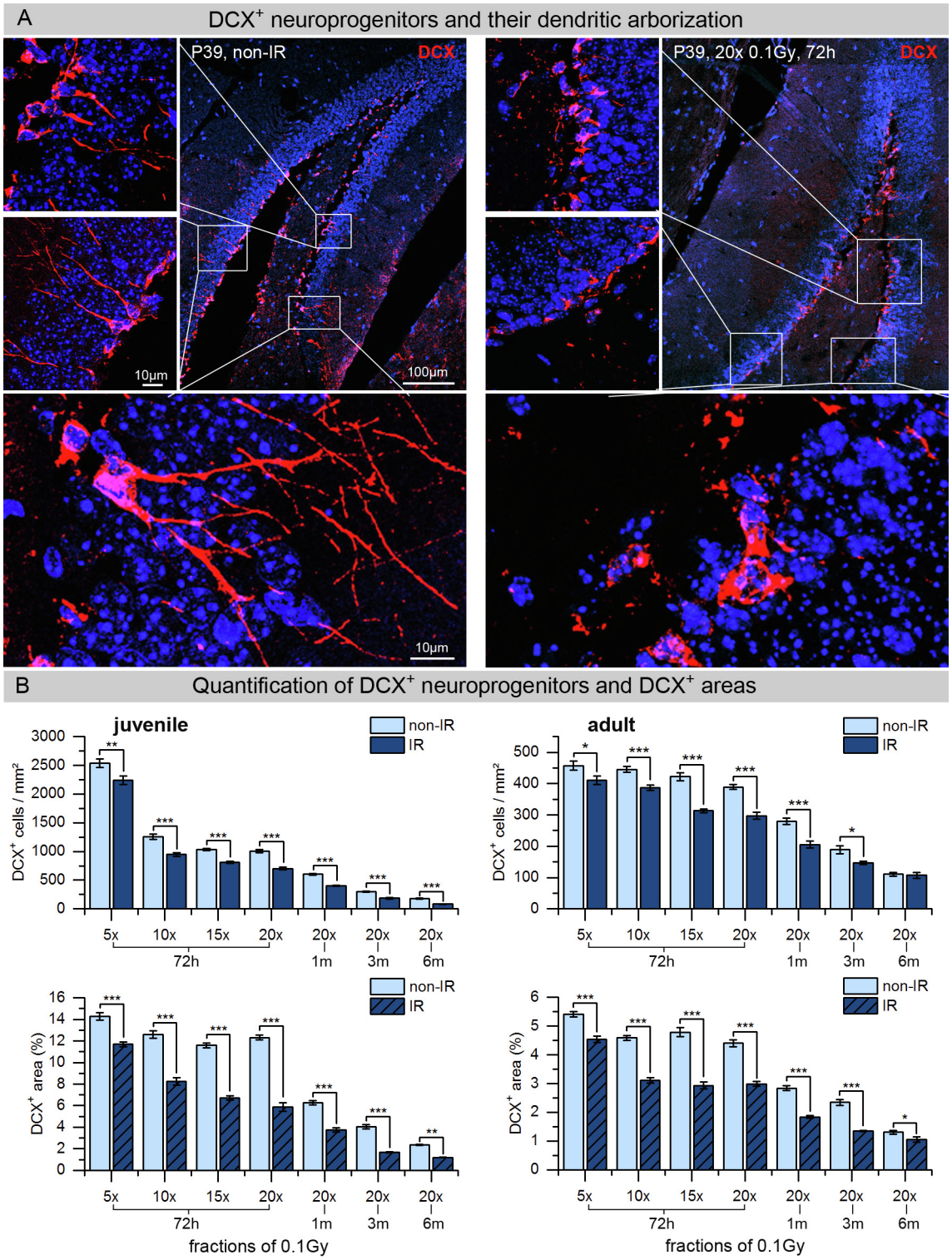

Fig. 2. DCX$^+$ neuroprogenitors and their dendritic arborization. A: Immunofluorescence imaging of DCX (red) in the dentate gyrus of non-irradiated (left panel) and irradiated (20 × 0.1 Gy, 72 h) hippocampus (right panel) from juvenile WT mice. DCX$^+$ precursor cells are abundant in the SGZ of the dentate gyrus and show intact dendritic arborization. Framed regions are shown at higher magnification (600×). Projections of confocal *z*-stacks show that DCX$^+$ precursors after fractionated LDR are characterized by an impaired maturation of their dendritic tree. B: In the hippocampus of juvenile and adult WT mice the numbers of DCX$^+$ cells and DCX$^+$ area were quantified 72 h after 5×, 10×, 15×, or 20× fractions of 0.1 Gy and 1, 3, and 6 months after 20 × 0.1 Gy, in comparison to age-matched, non-irradiated controls. Error bars represent SEM, $n \geq 3$; *denotes statistically significant difference compared to non-irradiated control: $^{*}p < 0.05$; $^{**}p < 0.01$; $^{***}p < 0.001$.

immature neurons were clearly reduced before and after repetitive LDR (AT: 30–55 cells/mm^2; WT: 300–450 cells/mm^2), suggesting that even low levels of genomic damage result in their apoptotic elimination (Fig. 4B, lower panel). In SCID mice, almost normal basal levels of DCX$^+$ neuroprogenitors were observed in non-irradiated hippocampus (385 ± 6 cells/mm^2), while DCX$^+$ cell numbers decreased to ~30% after 10 × 0.1 Gy (116 ± 23 cells/mm^2) and to ~10% after 20 × 0.1 Gy (39 ± 4 cells/mm^2) (Fig. 4B). These

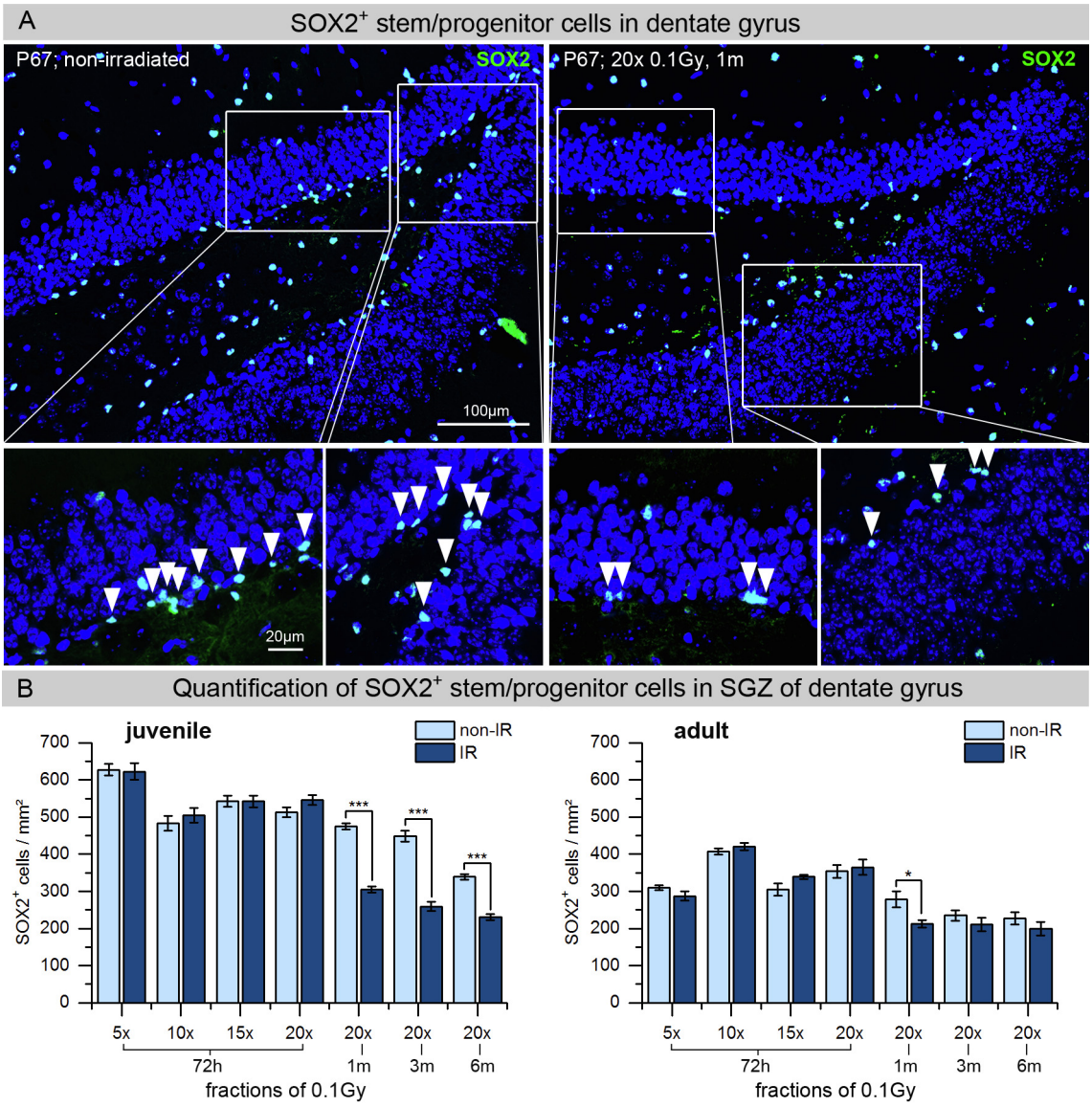

Fig. 3. SOX2$^+$ stem/progenitor cells in the SGZ of the dentate gyrus. A: Immunofluorescence imaging for SOX2 (green) in the dentate gyrus of non-irradiated (left panel) and irradiated (20 × 0.1 Gy, 1 m) hippocampus (right panel) from adult WT mice (P67). SOX2$^+$ cells in the SGZ represent neuronal stem cells. Framed regions are shown at higher magnification. Arrow heads mark SOX2$^+$ nuclei in the SGZ. Scale bars represent 100 µm or 20 µm, respectively. Original magnification 600×. B: In the hippocampus of juvenile and adult WT mice the numbers of SOX2$^+$ cells in the SGZ were quantified 72 h after 5×, 10×, 15×, 20× fractions of 0.1 Gy and 1, 3 and 6 months after 20 × 0.1 Gy, and compared to age-matched, non-irradiated controls. Error bars represent SEM, $n \geq 3$; *denotes statistically significant difference compared to non-irradiated control: $^*p < 0.05$; $^{**}p < 0.01$; $^{***}p < 0.001$.

findings suggest that excessive DNA damage leads to apoptotic elimination of DCX$^+$ neuroprogenitors due to their increased susceptibility. The number of slowly proliferating SOX2$^+$ cells, by contrast, remained stable during fractionated LDR throughout the different mouse strains.

Fractionated LDR affects the hippocampal proteome

Analysis of hippocampal proteome of juvenile WT mice was performed 72 h, 1, 3 and 6 months after fractionated LDR (20 × 0.1 Gy). Label-free LC/MS-MS was used for comparison of irradiated hippocampus versus age-matched, non-irradiated controls. Volcano plots of all quantified proteins show the distribution of non-regulated and deregulated proteins (Fig. 5A). Total numbers of significantly down- and up-regulated proteins are shown in Fig. 5B. At 72 h post-IR, most proteins were down-regulated, whereas at 1 m post-IR most proteins were up-regulated. At later time-points, the distribution of down- and up-regulated proteins was almost equal. Shared proteins are presented in the Venn diagram (Fig. 5C).

Pathway analysis indicates the modulation of CREB signaling

Deregulated proteins were further analyzed using Ingenuity Pathway Analysis (IPA) software. Most affected signaling pathways were synaptic long-term potentiation and CREB signaling, both of which are important in neuronal functioning (Suppl.2). Transcription-factor CREB is activated by phosphorylation of Ser133 via calmodulin kinases (CAMKs). Based on proteomics data, CAMKs were down-regulated at 72 h and 1 m post-IR, but up-regulated at 3 m post-IR (Suppl.2). Predicted changes in CREB-pathway were validated using immunoblotting. Levels of

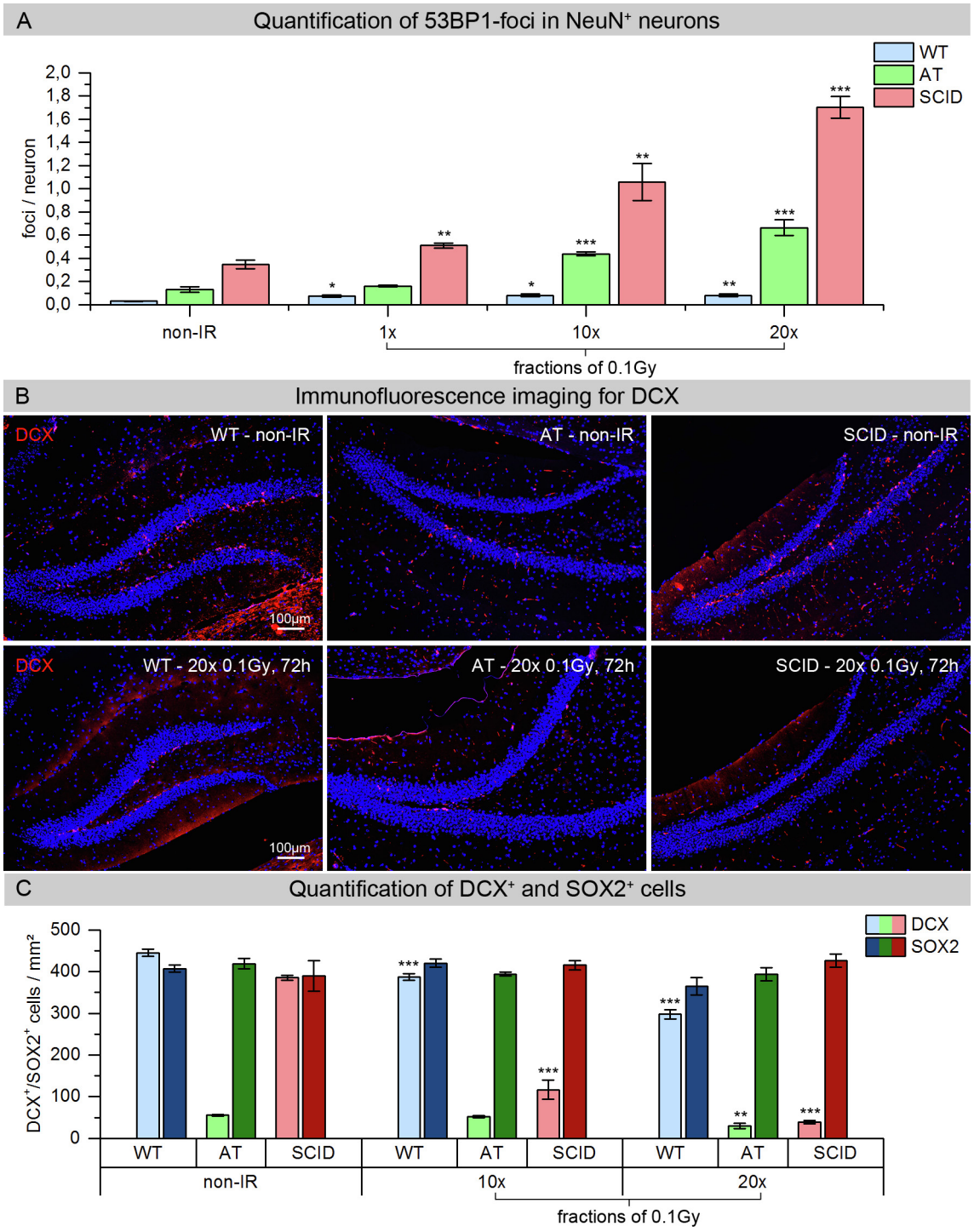

Fig. 4. Effect of DNA damage accumulation on adult neurogenesis A: Quantification of 53BP1-foci in hippocampal neurons 72 h after 1×, 10× and 20× fractions of 0.1 Gy in WT. AT and SCID mice, compared to non-irradiated controls. B: Immunofluorescence imaging for DCX in the dentate gyrus of non-irradiated and irradiated (20 × 0.1 Gy, 72 h) hippocampus from adult WT, AT and SCID mice. C: Quantification of DCX⁺ and SOX2⁺ cells in the SGZ of dentate gyrus of WT, AT and SCID mice performed 72 h after the last exposure of fractionated LDR (10× and 20× fractions of 0.1 Gy). Error bars represent SEM, $n \geq 3$; *denotes statistically significant difference compared to non-irradiated control: * $p < 0.05$; ** $p < 0.01$; *** $p < 0.001$.

phosphorylated (Ser133) and total-CREB, and the downstream targets BDNF and ARC are shown in Fig. 6. Down-regulation of phospho-CREB (pCREB) at 72 h and 1 m post-IR and up-regulation at 3 m post-IR is in line with simultaneous down- and up-regulation of CAMKs (Suppl.2). In agreement with pCREB deregulation, the downstream targets BDNF and ARC were significantly downregulated at 1 m post-IR and upregulated at 3 m post-IR (Fig. 6). Down-regulation of CREB-signaling directly after LDR suggests that radiation-induced genotoxic insults suppress hippocampal neurogenesis, whereas late-term CREB-activation may stimulate neuronal cell proliferation/differentiation and promote functional regeneration after genotoxic stress.

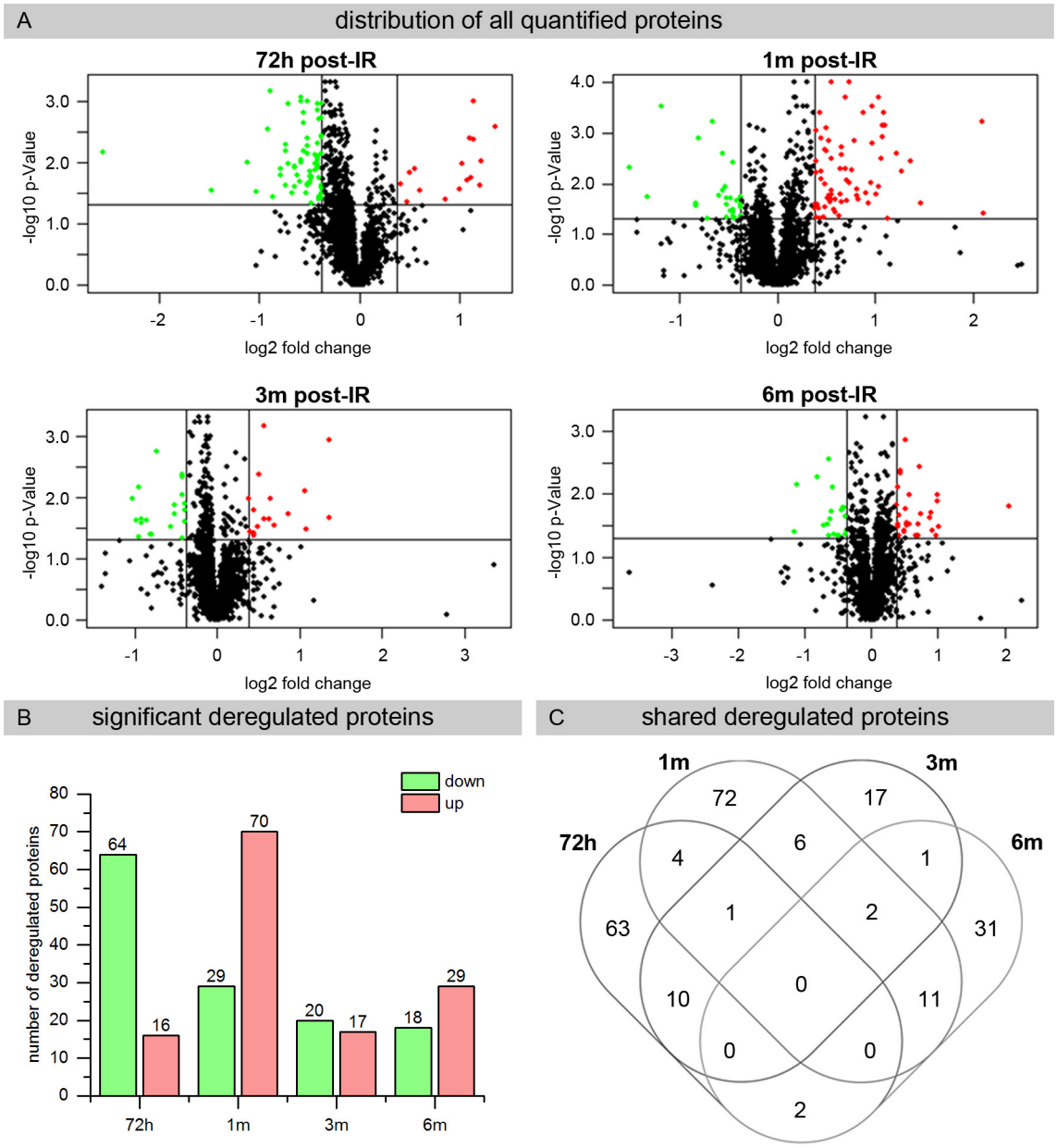

Fig. 5. Analysis of the hippocampal proteome. A: Volcano plots representing the distribution of all quantified proteins (identification with ≥ 2 UP) at 72 h, 1, 3 and 6 months post-IR (20 × 0.1 Gy). Deregulated proteins ($p \leq 0.05$, fold change ± 1.3) are highlighted in green (down-regulated) and red (up-regulated), respectively. B: Total numbers of significantly down-regulated (green) and up-regulated (red) proteins are shown for all time points ($p \leq 0.05$, fold change ± 1.3). C: Venn diagram illustrates the number of shared deregulated proteins at different time-points.

Discussion

The high hippocampal susceptibility to radiation injury is likely the causal factor of neurocognitive dysfunctions after exposure to ionizing radiation [25]. To analyze the impact of repeated low-dose exposure on hippocampal neurogenesis, we utilized an *in-vivo* model, exposing genetically determined mouse strains with different DNA repair capacities to daily LDR. During this LDR regime mice were irradiated with 0.1 Gy every day (except weekends) for up to 4 weeks. Fractionated LDR enclosing only the head of every single animal is very laborious and time-consuming and would require daily narcosis for immobilization. The risks and side effects of daily anesthesia would clearly exceed the benefits of the selective brain irradiation, especially for young animals. Depending on their DNA repair capacity, repeated LDR led to varying levels of persisting DNA damage foci in hippocampal neurons with increasing cumulative doses [22]. As a result of radiation-induced DNA damage accumulation hippocampal neurogenesis was seriously affected in DNA repair-deficient mice [26]. But even in repair-proficient WT mice, radiation-induced genotoxic stress resulted in progressive reduction in DCX^+ immature neurons with impairment in their dendritic development. Importantly, following completion of fractionated LDR, DCX^+ and $SOX2^+$ cells exhibited significant long-lasting decline within their neurogenic niche, which was even more pronounced in juvenile brain.

The response of tissue-specific stem/progenitor cells to radiation exposure is an important determinant of overall tissue reaction. During the process of adult neurogenesis, heterogenous mixtures of neuronal stem/precursors cells undergo numerous proliferation and differentiation stages. Our findings indicate that different subpopulations of neuronal stem/progenitor cells respond differently to fractionated LDR. The number of DCX^+

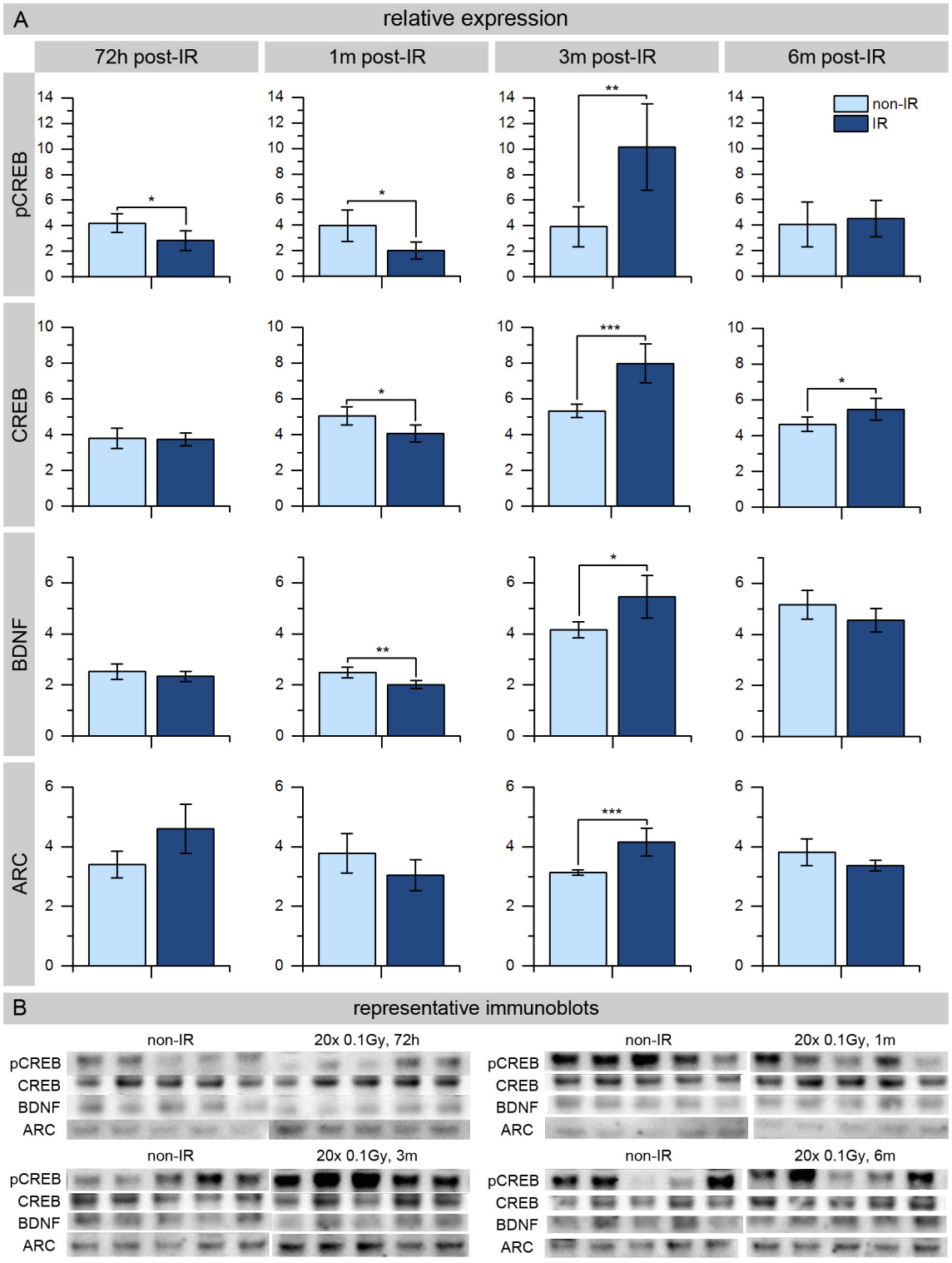

Fig. 6. Immunoblot analysis of phospho- and total-CREB levels and the downstream targets BDNF and ARC. The relative expression of phospho-CREB (Ser133), CREB, BDNF and ARC at 72 h, 1, 3 and 6 months post-IR (20 × 0.1 Gy) compared to non-irradiated, age-matched controls, after background correction and normalization to total amount of protein visualized by Ponceau staining. Error bars represent SEM, $n \geq 3$; *denotes statistically significant difference compared to non-irradiated control: $^{*}p < 0.05$; $^{**}p < 0.01$; $^{***}p < 0.001$.

dividing progenitor cells and the complexity of their dendritic architectures gradually declined during and after LDR, likely due to radiation-induced suppression of proliferation and maturation. The number of SOX2^{+} stem/progenitor cells remained constant during LDR, but decreased significantly within several months after LDR. Regenerative processes necessitate stem cell replication with enhanced differentiation/maturation to replace damaged cells after radiation injury [27]. Excessive activation of stem/progenitor cells by genotoxic insults may result in premature exhaustion of stem cells [20,28]. Our results suggest that this dynamic balance within the stem cell pool is critically influenced by repeated small doses of ionizing radiation. Higher proportions of proliferating

neuroprogenitors in juvenile hippocampus may explain the increased radiosusceptibility of young organisms [29]. This study provides the basis for future experiments designed to assess neurogenesis and neuroinflammation by the combination of immunocytochemistry with stereological techniques to estimate exactly the numbers of different cell populations in defined brain volumes after radiation-mediated damage.

Label-free quantitative proteomics based on mass spectrometry is an important approach for exploring protein functions and interactions in a large-scale manner. Since the isolation of specific regions is not feasible in unstained tissue, we used the whole hippocampus for proteomics analysis. Label-free LC–MS/MS technology is not sensitive enough to identify very weekly expressed proteins such as transcription factors. Nevertheless, based on protein profiling, the activation status of central transcriptional regulators can be predicted using specific software tools. In this study, the predicted changes in the active form of transcription factor CREB were followed by performing immunoblotting. Our hippocampal proteome analysis revealed the importance of CREB-mediated gene transcription in radiation response, with CREB-target proteins BDNF and ARC promoting neuronal maturation with outgrowth of axons and dendrites [30,31]. Down-regulation of CREB-signaling directly after LDR correlates with suppression of hippocampal neurogenesis. CREB-mediated up-regulation of neurotrophic factors suggest functional recovery of neurogenesis several months after fractionated LDR [32].

In summary, these results enhance our understanding of molecular and cellular dynamics that underlie hippocampal neurogenesis during and after fractionated LDR. Our experimental data indicate that fractionated LDR impairs neurogenesis, and may compromise hippocampus-dependent learning and memory. Markedly, our findings suggest that repeated LDR leads to persistent injury of hippocampal neurogenesis, even more pronounced in young individuals [33]. In future studies, cognitive functioning will be tested in this mouse model of fractionated LDR to assess potential radiation-induced deficits. This experimental study provides a framework for clinical radiotherapy, with recommendation for significant dose reduction in hippocampus regions whenever possible to prevent neuro-cognitive dysfunction.

Conflicts of interest

The authors declare no potential conflicts of interest.

Acknowledgement

The authors acknowledge the technical assistance of Dr. Eric Hummel, Carl Zeiss Microscopy GmbH, for high-resolution imaging and Kathrin Förderer for performing animal experiments.

Research grants

The research leading to these results has received funding from the Federal Ministry of Education and Research (BMBF), Germany under ther reference numbers 02NUK035A (Claudia E. Rübe) and 02NUK045C (Soile Tapio).

Appendix A. Supplementary data

Supplementary data to this article can be found online at https://doi.org/10.1016/j.radonc.2019.04.021.

References

[1] Padovani L, Andre N, Constine LS, Muracciole X. Neurocognitive function after radiotherapy for paediatric brain tumours. Nat Rev Neurol 2012;8:578–88.
[2] Acharya MM, Patel NH, Craver BM, Tran KK, Giedzinski E, Tseng BP, et al. Consequences of low dose ionizing radiation exposure on the hippocampal microenvironment. PLoS One 2015;10:e0128316.
[3] Parihar VK, Limoli CL. Cranial irradiation compromises neuronal architecture in the hippocampus. Proc Natl Acad Sci USA 2013;110:12822–7.
[4] Rao AA, Ye H, Decker PA, Howe CL, Wetmore C. Therapeutic doses of cranial irradiation induce hippocampus-dependent cognitive deficits in young mice. J Neurooncol 2011;105:191–8.
[5] Rola R, Fishman K, Baure J, Rosi S, Lamborn KR, Obenaus A, et al. Hippocampal neurogenesis and neuroinflammation after cranial irradiation with (56)Fe particles. Radiat Res 2008;169:626–32.
[6] Schindler MK, Bourland JD, Forbes ME, Hua K, Riddle DR. Neurobiological responses to stereotactic focal irradiation of the adult rodent hippocampus. J Neurol Sci 2011;306:129–37.
[7] Tang FR, Loke WK, Khoo BC. Postnatal irradiation-induced hippocampal neuropathology, cognitive impairment and aging. Brain Dev 2017;39:277–93.
[8] Kempermann G, Song H, Gage FH. Neurogenesis in the Adult Hippocampus. Cold Spring Harb Perspect Biol 2015;7:a018812.
[9] Amador-Arjona A, Cimadamore F, Huang CT, Wright R, Lewis S, Gage FH, et al. SOX2 primes the epigenetic landscape in neural precursors enabling proper gene activation during hippocampal neurogenesis. Proc Natl Acad Sci USA 2015;112:E1936–45.
[10] von Bohlen Und Halbach O. Immunohistological markers for staging neurogenesis in adult hippocampus. Cell Tissue Res 2007;329:409–20.
[11] Gusel'nikova VV, Korzhevskiy DE. NeuN As a Neuronal Nuclear Antigen and Neuron Differentiation Marker. Acta Naturae 2015;7:42–7.
[12] Semple BD, Blomgren K, Gimlin K, Ferriero DM, Noble-Haeusslein LJ. Brain development in rodents and humans: Identifying benchmarks of maturation and vulnerability to injury across species. Prog Neurobiol 2013;106–107:1–16.
[13] Urban N, Guillemot F. Neurogenesis in the embryonic and adult brain: same regulators, different roles. Front Cell Neurosci 2014;8:396.
[14] Merz K, Herold S, Lie DC. CREB in adult neurogenesis–master and partner in the development of adult-born neurons? Eur J Neurosci 2011;33:1078–86.
[15] Panja D, Bramham CR. BDNF mechanisms in late LTP formation: A synthesis and breakdown. Neuropharmacology 2014:664–76.
[16] Li Y, Pehrson AL, Waller JA, Dale E, Sanchez C, Gulinello M. A critical evaluation of the activity-regulated cytoskeleton-associated protein (Arc/Arg3.1)'s putative role in regulating dendritic plasticity, cognitive processes, and mood in animal models of depression. Front Neurosci 2015;9:279.
[17] Rothkamm K, Barnard S, Moquet J, Ellender M, Rana Z, Burdak-Rothkamm S. DNA damage foci: Meaning and significance. Environ Mol Mutagen 2015;56:491–504.
[18] Shiloh Y, Ziv Y. The ATM protein kinase: regulating the cellular response to genotoxic stress, and more. Nat Rev Mol Cell Biol 2013;14:197–210.
[19] Chang C, Biedermann KA, Mezzina M, Brown JM. Characterization of the DNA double strand break repair defect in scid mice. Cancer Res 1993;53:1244–8.
[20] Behrens A, van Deursen JM, Rudolph KL, Schumacher B. Impact of genomic damage and ageing on stem cell function. Nat Cell Biol 2014;16:201–7.
[21] Tang FR, Loke WK, Khoo BC. Low-dose or low-dose-rate ionizing radiation-induced bioeffects in animal models. J Radiat Res 2017;58:165–82.
[22] Lorat Y, Schanz S, Rube CE. Ultrastructural insights into the biological significance of persisting DNA Damage foci after low doses of ionizing radiation. Clin Cancer Res 2016;22:5300–11.
[23] Wisniewski JR, Zougman A, Nagaraj N, Mann M. Universal sample preparation method for proteome analysis. Nat Methods 2009;6:359–62.
[24] Grosche A, Hauser A, Lepper MF, Mayo R, von Toerne C, Merl-Pham J, et al. The proteome of native adult muller glial cells from murine retina. Mol Cell Proteomics 2016;15:462–80.
[25] Hladik D, Tapio S. Effects of ionizing radiation on the mammalian brain. Mutat Res 2016;770:219–30.
[26] Enriquez-Rios V, Dumitrache LC, Downing SM, Li Y, Brown EJ, Russell HR, et al. DNA-PKcs, ATM, and ATR interplay maintains genome integrity during neurogenesis. J Neurosci 2017;37:893–905.
[27] Favaro R, Valotta M, Ferri AL, Latorre E, Mariani J, Giachino C, et al. Hippocampal development and neural stem cell maintenance require Sox2-dependent regulation of Shh. Nat Neurosci 2009;12:1248–56.
[28] Schuler N, Timm S, Rube CE. Hair follicle stem cell faith is dependent on chromatin remodeling capacity following low-dose radiation. Stem Cells 2018;36:574–88.
[29] Hudson D, Kovalchuk I, Koturbash I, Kolb B, Martin OA, Kovalchuk O. Induction and persistence of radiation-induced DNA damage is more pronounced in young animals than in old animals. Aging (Albany NY) 2011;3:609–20.
[30] Leal G, Comprido D, Duarte CB. BDNF-induced local protein synthesis and synaptic plasticity. Neuropharmacology 2014:639–56.
[31] Sauvage MM, Nakamura NH, Beer Z. Mapping memory function in the medial temporal lobe with the immediate-early gene Arc. Behav Brain Res 2013;254:22–33.
[32] Hwang IK, Yoo KY, Yoo DY, Choi JW, Lee CH, Choi JH, et al. Time-course of changes in phosphorylated CREB in neuroblasts and BDNF in the mouse dentate gyrus at early postnatal stages. Cell Mol Neurobiol 2011;31:669–74.
[33] Casciati A, Dobos K, Antonelli F, Benedek A, Kempf SJ, Belles M, et al. Age-related effects of X-ray irradiation on mouse hippocampus. Oncotarget 2016;7:28.